Ga_2O_3 Schottky rectifiers with 1 ampere forward current, 650 V reverse breakdown and 26.5 MW.cm^{-2} figure-of-merit

Cite as: AIP Advances **8**, 055026 (2018); https://doi.org/10.1063/1.5034444
Submitted: 11 April 2018 . Accepted: 16 May 2018 . Published Online: 24 May 2018

Jiancheng Yang, F. Ren, Marko Tadjer, S. J. Pearton, and A. Kuramata

Ga_2O_3 Schottky rectifiers with 1 ampere forward current, 650 V reverse breakdown and 26.5 MW.cm^{-2} figure-of-merit

Jiancheng Yang,[1] F. Ren,[1] Marko Tadjer,[2] S. J. Pearton,[3,a] and A. Kuramata[4]
[1]*Department of Chemical Engineering, University of Florida, Gainesville, FL 32611, USA*
[2]*Naval Research Laboratory, Washington, DC 20375, USA*
[3]*Department of Materials Science and Engineering, University of Florida, Gainesville, FL 32611, USA*
[4]*Tamura Corporation and Novel Crystal Technology, Inc., Sayama, Saitama 350-1328, Japan*

(Received 11 April 2018; accepted 16 May 2018; published online 24 May 2018)

A key goal for Ga_2O_3 rectifiers is to achieve high forward currents and high reverse breakdown voltages. Field-plated β-Ga_2O_3 Schottky rectifiers with area 0.01 cm^2, fabricated on 10 μm thick, lightly-doped drift regions (1.33 x 10^{16} cm^{-3}) on heavily-doped (3.6 x 10^{18} cm^{-3}) substrates, exhibited forward current density of 100A.cm^{-2} at 2.1 V, with absolute current of 1 A at this voltage and a reverse breakdown voltage (V_B) of 650V. The on-resistance (R_{ON}) was 1.58 x 10^{-2} Ω.cm^2, producing a figure of merit (V_B^2/R_{ON}) of 26.5 MW.cm^{-2}. The Schottky barrier height of the Ni was 1.04 eV, with an ideality factor of 1.02. The on/off ratio was in the range 3.3 x 10^6 - 5.7 x 10^9 for reverse biases between 5 and 100V. The reverse recovery time was ~30 ns for switching from +2V to -5V. The results show the capability of β-Ga_2O_3 rectifiers to achieve exceptional performance in both forward and reverse bias conditions. https://doi.org/10.1063/1.5034444

There is significant interest in power electronics based on β-Ga_2O_3 because it has a larger potential figure-of-merit than GaN and SiC for some of the applications needed for low frequency, high voltage power switching.[1–5] These applications generally require a high electric field breakdown strength, low on-state resistance (R_{on}) and low charge storage times. The operation of power wide bandgap semiconductor devices is constrained by this critical electric field for breakdown.[6] Empirically, the actual resistance is proportional to a power law of the breakdown voltage ($V_B^{2.3-2.5}$) as a result of a decrease in breakdown field strength in lightly doped drift layers that support the electric field.[7] A higher value of R_{on} increases conduction loss and lowers switching speed. Recent reviews on advances in device technologies have detailed the reasons for the interest in Ga_2O_3, revolving around its large bandgap (~4.8 eV), wide range of controlled n-type doping concentrations during bulk or epitaxial growth and availability of high quality, large diameter substrates.[1–5]

Schottky diode rectifiers are key components for power conversion. Operation of Schottky rectifiers up to 2MHz allows more efficient design of switch-mode power converters via a decrease in the size of the passive elements.[8,9] The dimensions of the passive elements, specifically the transformers, filters, capacitors and inductors, inversely scale with frequency of operation.[7,9] Many recent examples of impressive performance from Schottky rectifiers fabricated on Ga_2O_3 have appeared.[10–19] In particular, since the rapid progress in epitaxial growth methods for Ga_2O_3, most rectifier designs now employ a lightly doped drift layer grown on a conducting bulk wafer. The breakdown voltage can be enhanced using edge termination methods that reduce field crowding at the edge of the Schottky contact.[14,16] Avalanche breakdown, which occurs under a high electric field, is typically observed around the edge of the gate electrode during the operation of the rectifier. The peak electric field that is concentrated on the edge of the gate electrode can be alleviated by the introduction of a field plate.

[a]Electronic mail: spear@mse.ufl.edu

In terms of rectifiers on bulk substrates, He et al.[11] achieved a forward current density of 421 A/cm^2 at 2 V, R_{on} of 2.9 mΩ· cm^2, and reverse recovery time of 20 ns. Half-wave rectification of ac voltages at different frequencies showed the rectifiers worked to 100 kHz. For rectifiers on epi Ga_2O_3, Konishi et al.[14] reported 1kV field-plated Schottky diodes with specific on-resistance of 5.1 mΩ.cm^2 for anode diameters of 200-400 μm. The type of dielectric material, its thickness, ramp angle and the extent of metal overlap onto the field plate all influence the effectiveness of the field reduction. Most of the field plates employed have been simple SiO_2 or SiN_X. Bae et al.[17] employed novel BN field plates on quasi-two-dimensional β-Ga_2O_3 field effect transistors to improve the off-state breakdown voltage. The key aspect in designing the field plate edge termination is to shift the region of the high field region away from the periphery of the rectifying contact. Yang et al.[12,13] reported breakdown voltages of 1.6 kV in vertical devices without edge termination. Finally, Oh et al.[18] reported characteristics of rectifiers up to 225°C, demonstrating their potential for effective, uncooled operation. For power conversion applications, the 600V market is one now accessed by GaN and SiC, with superior performance to Si devices.[20] Thus, achievement of breakdown voltage of >600V in Ga_2O_3 rectifiers with practical size and large absolute currents (not current density) is a milestone.

In all of the work to date, there has been a focus on either high reverse breakdown voltage or low on-resistance, in other words, emphasizing either the reverse or forward bias performance. It is obviously important to have good characteristics for both bias polarities. In this letter, we show that edge terminated Schottky rectifiers on low-doped epitaxial layers of β-Ga_2O_3 on bulk conducting substrates can achieve forward currents of 1 A at 2.1 V and reverse breakdown voltages of 650 V for relatively large (0.01 cm^2) devices.

The starting material consisted of epitaxial layers (10 μm final thickness) of lightly Si-doped n-type (1.33 x 10^{16} cm^{-3}) Ga_2O_3 grown by Hydride Vapor Phase Epitaxy (HVPE) on n$^+$ (3.6 x 10^{18} cm^{-3}), β-phase Sn-doped Ga_2O_3 single crystal wafers (~650 μm thick) with (001) surface orientation (Tamura Corporation, Japan) grown by the edge-defined film-fed method. The epitaxial layers were planarized by chemical mechanical planarization and the back surface of the substrate also polished to remove sub-surface damage and enhance Ohmic contact formation.

Diodes were fabricated by depositing full area back Ohmic contacts of Ti/Au (20 nm/80 nm) by E-beam evaporation, followed by rapid thermal annealing at 550°C for 30 seconds under N_2. The epi surface was treated with ozone for 10 minutes to remove carbon contamination and then a 100 nm thick SiN_x layer was deposited by plasma enhanced chemical vapor deposition at 300°C using silane and ammonia precursors. These SiN_x contact windows were patterned using lithography, and opened with 1:10 buffered oxide etch (BOE) solution at room temperature. The front side Schottky contacts were overlapped 10 μm on the SiN_x window openings by lift-off of E-beam deposited Ni/Au (40 nm/160 nm). The size of these contacts was 0.1 cm × 0.1 cm. Figure 1 shows a schematic of the rectifier structure (top), while an optical microscope plan view of the rectifying contact surrounded by the SiN_x field plate is shown at the bottom of the figure. Capacitance-voltage (C-V) characteristics were recorded in air at 25°C on an Agilent 4145B parameter analyzer and 4284A Precision LCR Meter. Current-voltage (I-V) characteristics were recorded in air at 25 °C using either an Agilent 4145B parameter analyzer or a Tektronix 370A curve tracer. The reverse breakdown voltage was defined as the voltage at which the reverse current was 1mA.cm^{-2}. This is a more useful definition than where the current sharply increases, since the latter depends on conduction mechanism. The 1mA.cm^{-2} definition allows meaningful comparison between different devices.

Figure 2 shows the C^{-2}-V characteristics used to confirm the drift layer n-type donor concentrations (N_D) from the slope of this plot. The value of 1.33 x 10^{16} cm^{-3} shows that the epitaxial layers of β-Ga_2O_3 can be controllably doped at low enough levels to sustain a large reverse bias while still having good forward characteristics. The single sweep forward current density characteristic is shown in Figure 3, reaching a current density of 100 A.cm^{-2} at 2.1 V. The specific on-state resistance of unipolar diode is a sum of the drift region resistance, the contact resistance and the substrate resistance,[9] ie.

$$R_{diode} = R_{drift} + R_{sub} + R_{contact}$$

The specific on-state resistance of the drift region is given by

$$R_{ON} = \int \frac{dx}{q\mu N_B} = \frac{W_D}{q\mu N_B}$$

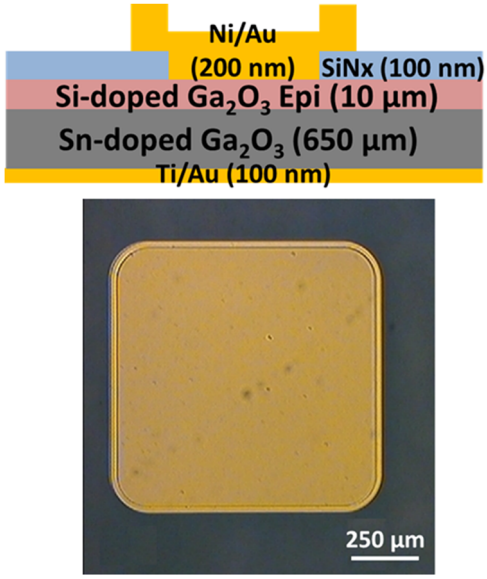

FIG. 1. Schematic of edge–terminated, vertical geometry Ni/Au Schottky rectifier structure (top) and top-view optical microscope image of completed device showing Ni/Au contact on SiN_x edge termination layer. The device area is 0.01 cm^2.

where μ is the low-field mobility (μ~300 $cm^2V^{-1}s^{-1}$ for Ga_2O_3),[20,21] N_D is the doping concentration in the drift region and W_D is the drift region thickness. We obtained an R_{ON} value of 1.58 x 10^{-2} Ω.cm^2 from the data in the inset of Figure 3. We have found that the on-resistance is a strong function of device size, ranging from 5.9x10^{-4}- 0.26 Ω.cm^2 for areas in the corresponding range 1.6x10^{-5}-0.2 cm^2. Note that the main plot is collected using the Tektronix tool, and the current limit is scaled with the measurement range. For our measurements, we were measuring the current range of 1 amp, and the Tektronix tool has a lower limit of 5 mA on this scale. The insert figure in that plot is collected by the Agilent 4156, where we can measure current down to the pA range.

For these moderately doped layers, the dominant current transport process in Schottky contacts will be thermionic emission. If the current flow is dominated by thermionic emission, then the ideality factor *n* should be close to unity, with a small increase from unity due to the image force effect.[14] For extraction of the barrier height from these characteristics, we fitted the linear portions that obeyed the ideal thermionic-emission behavior. We obtained an ideality factor of 1.02 and a barrier height of 1.04 eV. The latter is consistent with literature values for Ni on Ga_2O_3.[21–32] Konishi et al.[14] have

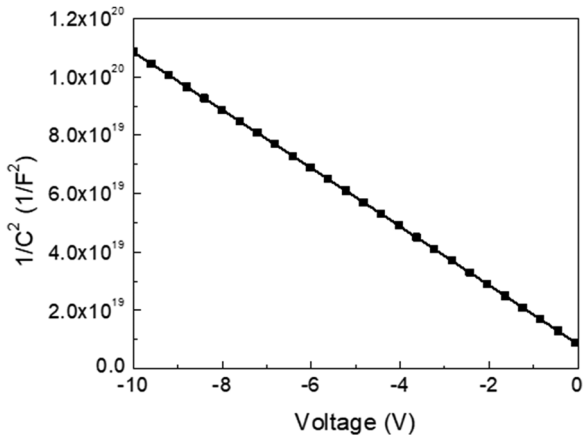

FIG. 2. C^{-2}-V characteristic, revealing a drift layer carrier concentration of 1.33 x10^{16} cm^{-3}.

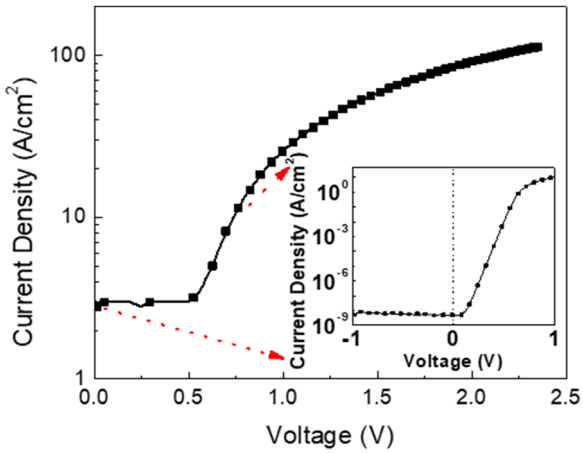

FIG. 3. Forward current density-voltage characteristic of rectifier shown on log scale.

noted that prolonged exposure of the surface to fluorine-containing chemicals or gases (eg. HF) may increase the effective barrier height through F^- compensation of donors in the near-surface region. We have recently confirmed that Fluorine is incorporated at high concentrations into Ga_2O_3 and is present in at least two forms.[33] These are a fairly immobile, high concentration form that is likely to be

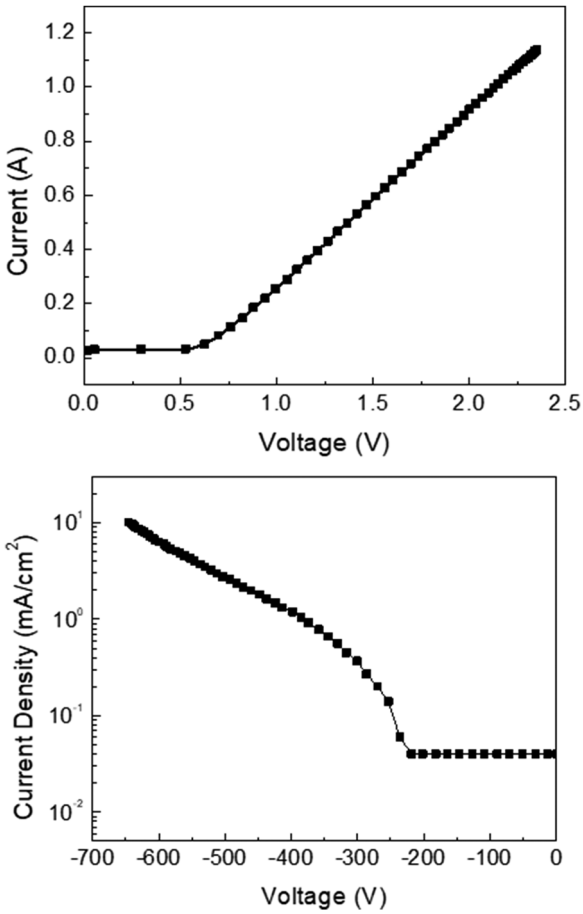

FIG. 4. Forward (top) and reverse (bottom) I-V characteristics shown on linear scale.

molecules and the other is atomic fluorine that can be ionized to compensate Si donors. The Schottky barrier heights are higher than reference samples due to the chemical influence of the fluorine.

Figure 4 (top) shows the forward current (I-V) characteristics on a linear scale, while 4 (bottom) shows the reverse current characteristic. The reverse breakdown voltage is 650 V, leading to a figure of merit (V_B^2/R_{ON}) of 26.5 MW.cm^{-2}. This is well below the values of 102-154 MW.cm^{-2} reported for rectifiers with much smaller contacts (~100 μm diameter),[12,13] but in those devices, the total forward current was more than 3 orders of magnitude lower than achieved here. Similarly, the 650V breakdown voltage is consistent with the needs of medium power industry applications,[9] such as photovoltaics, wind, and motor drives. Increasing energy efficiency in every aspect of power consumption, power delivery, and power conversion is important in these applications.[9]

Figure 5 shows the on/off current ratio measured at a fixed forward bias of 3V and reverse biases of -1 to -100V. The on/off ratio varied from 3.3 x 10^9 to 5.67 x 10^6 over this range and better than our previous report,[13] which is likely due to continued improvement in epitaxial material doping control.

Figure 6 shows the reverse recovery characteristics when switching from +2V to -5V, with a recovery time of order 30 ns. This is comparable to previous reports with much smaller rectifier

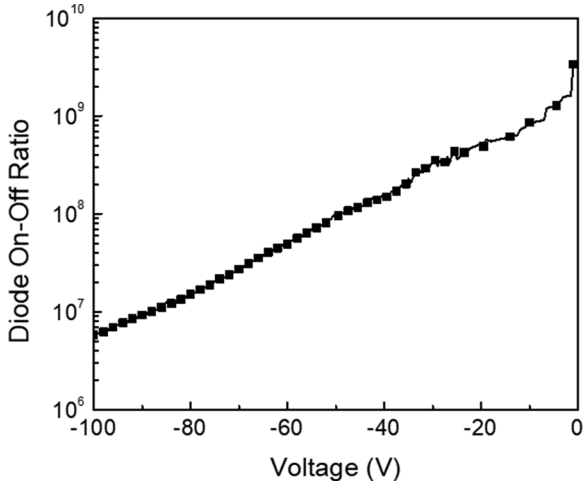

FIG. 5. Rectifier on-off ratio as a function of reverse bias. The on-current was 1 A at 3V and the on-off ration range measured was 3.3x10^9- 5.7x10^6.

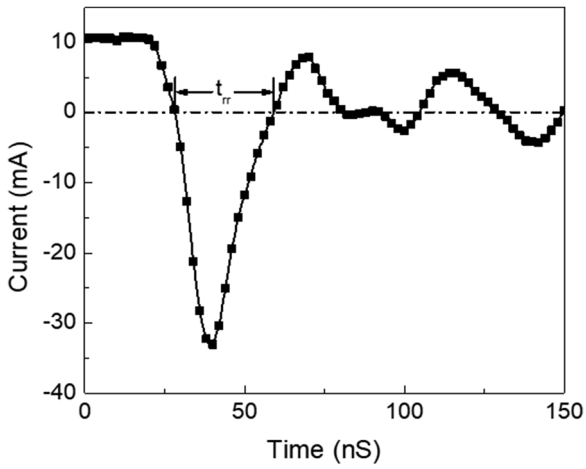

FIG. 6. Reverse recovery measurement when switching from +2 to -5 V.

dimensions.[12] These results show the potential of β-Ga_2O_3 for fast – switching power devices, capable of high on-state currents and breakdown voltages.

In summary, the availability of thick, lightly doped drift regions enable realization of large dimension (0.01 cm^2) β-Ga_2O_3 Schottky rectifiers with simultaneous large forward current (1A), V_{BR} values of 650 V and power density figures of merit above 20 $MW.cm^{-2}$. Since power converters require the power device to switch at high frequencies for improved dynamic response capability and reduced passive component size and weight, the performance of these Ga_2O_3 rectifiers is consistent with these goals. The present results show that β-Ga_2O_3 Schottky rectifiers are promising practical candidates for high power devices.

The project at UF was sponsored by the Department of the Defense, Defense Threat Reduction Agency, HDTRA1-17-1-011, monitored by Jacob Calkins. The content of the information does not necessarily reflect the position or the policy of the federal government, and no official endorsement should be inferred. Research at NRL was supported by the Office of Naval Research, partially under Award Number N00014-15-1-2392. Part of the work at Tamura was supported by "The research and development project for innovation technique of energy conservation" of the New Energy and Industrial Technology Development Organization (NEDO), Japan. Research at Novel Crystal Technology is partially supported by ONR Global (Grant # N62909-16-1-2217). We also thank Dr. Kohei Sasaki from Tamura Corporation for fruitful discussions.

[1] M. Higashiwaki and G. H. Jessen, Appl. Phys. Lett. **112**, 060401 (2018).
[2] H. Von Wenckstern, Adv. Electron. Mater. **3**, 1600350 (2017).
[3] J. Y. Tsao, S. Chowdhury, M. A. Hollis, D. Jena, N. M. Johnson, K. A. Jones, R. J. Kaplar, S. Rajan, C. G. Van de Walle, E. Bellotti, C. L. Chua, R. Collazo, M. E. Coltrin, J. A. Cooper, K. R. Evans, S. Graham, T. A. Grotjohn, E. R. Heller, M. Higashiwaki, M. S. Islam, P. W. Juodawlkis, M. A. Khan, A. D. Koehler, J. H. Leach, U. K. Mishra, R. J. Nemanich, R. C. N. Pilawa-Podgurski, J. B. Shealy, Z. Sitar, M. J. Tadjer, A. F. Witulski, M. Wraback, and J. A. Simmons, Adv. Electron. Mater. **4**, 1600501 (2018).
[4] S. J. Pearton, J. Yang, P. H. Cary IV, F. Ren, J. Kim, M. J. Tadjer, and M. A. Mastro, Appl. Phys. Rev. **5**, 011301 (2018).
[5] M. Higashiwaki, A. Kuramata, H. Murakami, and Y. Kumagai, J. Phys. D: Appl. Phys. **50**, 333002 (2017).
[6] T. Kimoto, Jap. J. Appl. Phys. **54**, 040103 (2015).
[7] B. Bayraktaroglu, Assessment of Gallium Oxide Technology, Air Force Research Lab, Devices for Sensing Branch, Aerospace Components & Subsystems Division, Report AFRL-RY-WP-TR-2017-0167 (2017).
[8] M. Mastro, "Power MOSFETs and diodes," in *Gallium Oxide-Technology, Devices and Applications*, ed. S. J. Pearton, F. Ren, and M. Mastro (Elsevier, London, 2018).
[9] A. Q. Huang, Proc. IEEE **105**, 2019 (2017).
[10] M. Higashiwaki, K. Konishi, K. Sasaki, K. Goto, K. Nomura, Q. T. Thieu, R. Togashi, H. Murakami, Y. Kumagai, B. Monemar, A. Koukitu, A. Kuramata, and S. Yamakoshi, Appl. Phys. Lett. **108**, 133503 (2016).
[11] Q. He, W. Mu, H. Dong, S. Long, Z. Jia, H. Lv, Q. Liu, M. Tang, X. Tao, and M. Liu, Appl. Phys. Lett. **110**, 093503 (2017).
[12] J. Yang, S. Ahn, F. Ren, S. J. Pearton, S. Jang, J. Kim, and A. Kuramata, Appl. Phys. Lett. **110**, 192101 (2017).
[13] J. Yang, S. Ahn, F. Ren, S. J. Pearton, S. Jang, and A. Kuramata, IEEE Electron Device Lett. **38**, 906 (2017).
[14] K. Konishi, K. Goto, H. Murakami, Y. Kumagai, A. Kuramata, S. Yamakoshi, and M. Higashiwaki, Appl. Phys. Lett. **110**, 103506 (2017).
[15] Q. He, W. Mu, B. Fu, Z. Jia, S. Long, Z. Yu, Z. Yao, W. Wang, H. Dong, Y. Qin, G. Jian, Y. Zhang, H. Xue, H. Lv, Q. Liu, M. Tang, X. Tao, and M. Liu, IEEE Electron Device Lett. **39**, 556 (2018).
[16] K. Sasaki, D. Wakimoto, Q. T. Thieu, Y. Koishikawa, A. Kuramata, M. Higashiwaki, and S. Yamakoshi, IEEE Electron Device Lett. **38**, 783 (2017).
[17] J. Bae, H. Woo Kim, I. Ho Kang, G. Yang, and J. Kim, Appl. Phys. Lett. **112**, 122102 (2018).
[18] S. Oh, G. Yang, and J. Kim, ECS J. Solid State Sci. Technol. **6**, Q3022 (2017).
[19] M. J. Tadjer, N. A. Mahadik, J. A. Freitas, E. R. Glaser, A. D. Koehler, L. E. Luna, B. N. Feigelson, K. D. Hobart, F. J. Kub, and A. Kuramata, SPIE Conf. Proc., Gallium Nitride Materials and Devices XIII, Vol. 10532, 1053212 (2018).
[20] H. Amano, Y. Baines, E. Beam, M. Borga, T. Bouchet, P. R. Chalker, M. Charles, K. J. Chen, N. Chowdhury, R. Chu, C. De Santi, M. M. De Souza, S. Decoutere, L. Di Cioccio, B. Eckardt, T. Egawa, P. Fay, J. J. Freedsman, L. Guido, O. Häberlen, G. Haynes, T. Heckel, D. Hemakumara, P. Houston, J. Hu, M. Hua, Q. Huang, A. Huang, S. Jiang, H. Kawai, D. Kinzer, M. Kuball, A. Kumar, K. B. Lee, X. Li, D. Marcon, M. März, R. McCarthy, G. Meneghesso, M. Meneghini, E. Morvan, A. Nakajima, E. M. S. Narayanan, S. Oliver, T. Palacios, D. Piedra, M. Plissonnier, R. Reddy, M. Sun, I. Thayne, A. Torres, N. Trivellin, V. Unni, M. J. Uren, M. Van Hove, D. J. Wallis, J. Wang, J. Xie, S. Yagi, S. Yang, C. Youtsey, R. Yu, E. Zanoni, S. Zeltner, and Y. Zhang, J. Phys. D: Appl. Phys. **51**, 163001 (2018).
[21] A. Parisi and R. Fornari, Semicond. Sci. Technol. **31**, 035305 (2016).
[22] K. Ghosh and U. Singisetti, J. Materials Research **32**, 4142 (2017).
[23] E. Ahmadi, Y. Oshim, F. Wu, and J. S. Speck, Semicond. Sci. Technol. **32**, 035004 (2017).
[24] K. Irmscher, Z. Galazka, M. Pietsch, R. Uecker, and R. Fornari, J. Appl. Phys. **110**, 063720 (2011).
[25] T. Oishi, Y. Koga, K. Harada, and M. Kasu, Appl. Phys. Express **8**, 031101 (2015).
[26] Y. Yao, R. Gangireddy, J. Kim, K. K. Das, R. F. Davis, and L. M. Porter, J. Vac. Sci. Technol. B **35**, 03D113 (2017).
[27] S. Ahn, F. Ren, L. Yuan, S. J. Pearton, and A. Kuramata, ECS J. Solid State Sci. Technol. **6**, P68 (2017).

[28] A. M. Armstrong, M. H. Crawford, A. Jayawardena, A. Ahyi, and S. Dhar, J. Appl. Phys. **119**, 103102 (2016).
[29] S. Oh, G. Yang, and J. Kim, ECS J. Solid State Sci. Technol. **2017**(6), Q3022 (2017).
[30] Z. Zhang, E. Farzana, A. R. Arehart, and S. A. Ringel, Appl. Phys. Lett. **108**, 052105 (2016).
[31] T. C. Lovejoy, R. Chen, X. Zheng, E. G. Villora, K. Shimamura, H. Yoshikawa, Y. Yamashita, S. Ueda, K. Kobayashi, S. T. Dunham, F. S. Ohuchi, and M. A. Olmstead, Appl. Phys. Lett. **100**, 181602 (2012).
[32] E. Farzana, Z. Zhang, P. K. Paul, A. R. Arehart, and S. A. Ringel, Appl. Phys. Lett. **111**, 202102 (2017).
[33] J. Yang, C. Fares, F. Ren, R. Sharma, E. Patrick, M. E. Law, S. J. Pearton, and A. Kuramata, J. Appl. Phys. **123**, 165706 (2018).